Nanoscale

Dynamic Article Links

Cite this: *Nanoscale*, 2012, **4**, 5931

www.rsc.org/nanoscale

PAPER

Tunable plasmon resonances in a metallic nanotip–film system†

Kazumasa Uetsuki,[a] Prabhat Verma,*[a] Peter Nordlander[b] and Satoshi Kawata[a]

Received 19th June 2012, Accepted 23rd July 2012
DOI: 10.1039/c2nr31542d

Tip-enhanced Raman spectroscopy (TERS) has emerged as a powerful tool for optical imaging at nanoscale spatial resolution, and for investigating the vibrational properties of molecules adsorbed on a substrate. Plasmonic enhancement of the electromagnetic fields near a metallic nanostructure plays a very important role in TERS, where resonant excitation of plasmons is crucial. When two metallic nanostructures are placed at a gap of nanometric distance, their plasmons can interact with one other and result in hybridized shifted plasmon modes. Here, we apply this idea to TERS and demonstrate a significant tunability of the plasmon resonance enabling large electric field enhancement at a desired excitation wavelength. This finding paves the way for efficient optimization of TERS in imaging and spectroscopy applications.

Introduction

The optical properties of metallic nanostructures have been extensively investigated because of their many important applications in spectroscopies and subwavelength waveguiding,[1,2] and – more recently – in biological and medical sciences.[3,4] The interaction of light with metallic nanostructures can excite localized surface plasmon resonance (LSPR), which can confine and enhance the incident light field near the surface of the nanostructure. In spectroscopic applications, such as surface enhanced Raman scattering (SERS), the importance of plasmon resonances stems from the large plasmon induced electric field enhancements that can result in drastically enhanced Raman signal from nearby molecules. These field enhancements are particularly large for resonant excitation of the plasmon. Therefore an understanding of how to tune the plasmon resonance energies of metallic nanostructures is becoming an important topic in nanooptics.

The energy of a LSPR is strongly dependent on the size and geometry of the nanostructure.[5–7] In particular, the energy can be dramatically modified by the presence of an adjacent metallic nanostructure due to their plasmonic interaction and resulting hybridization.[7,8] Such plasmon hybridization has received attention in the recent past because it has significant potential for tuning the energy of the LSPR.[6–11] An additional advantage of plasmonic couplings is the large field enhancements that are induced in the junctions between metallic nanostructures and can enable single-molecule SERS.[12,13] These properties are particularly useful for scanning probe optical microscopies, such as tip-enhanced Raman spectroscopy (TERS).[14–17] If a metallic nanotip, which is generally utilized in TERS is brought close to a metallic surface and is illuminated by light, the tip LSPR starts to interact with the delocalized surface plasmons of the substrate. The energies of such hybridized modes have already got some attention in the recent past.[18–20] Apart from large field enhancements, the tip–film system also provides a strong field confinement due to the sharpness of the tip.[20–22] Although the tip–film system has abundant advantages in TERS applications, it has not been extensively studied in this context except for the effects of gap width on the enhancement and confinement of the plasmon induced electric fields.

In this Article, we present an experimental and theoretical investigation to understand how the thickness of the film influences the energy and field enhancements of the hybridized nanotip–film plasmon modes. We show that for a fixed gap width, these properties are strongly influenced by the film thickness. We also show that for a specific incident laser wavelength, the hybridized plasmon resonance can be tuned to overlap the energy of incident light and that the measured TERS signal is then maximal. The tuning mechanism introduced by controlling the thickness of the metallic film can be exploited to optimize TERS geometries for general systems.

The plasmonic interaction between metallic nanoparticles and adjacent metallic films has been studied extensively,[9–11,23–29] and is here discussed only briefly. The interaction depends on the relative size of the nanoparticle and the thickness of the film. For a film with large thickness, the interaction is reflective of the dipole image, resulting in a redshift of the plasmon resonances with decreasing particle surface separation. However, for films with intermediate and small thicknesses where the dipole image of the nanoparticle does not fit inside the film, the plasmonic

[a]*Department of Applied Physics, Osaka University, Yamadaoka 2-1, Suita, Osaka 565-0871, Japan. E-mail: verma@ap.eng.osaka-u.ac.jp; Tel: +81 6 6879 4710*

[b]*Department of Physics and Astronomy and the Laboratory of Nanophotonics, Rice University, 6100 Main Street, Houston, Texas 77005, USA*

† Electronic supplementary information (ESI) available. See DOI: 10.1039/c2nr31542d

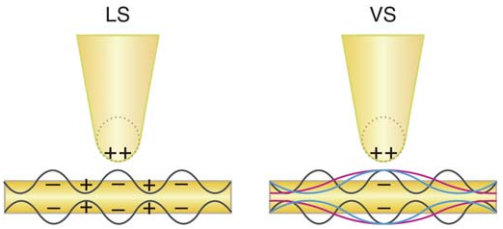

Fig. 1 Schematic models of charge distributions for the LS (left) and VS (right) modes in a metallic nanotip–film system. The higher energy LS mode only couples efficiently to short wavelength film plasmons while the VS couples to longer wavelength film plasmons as illustrated by the three differently colored film plasmon modes.

response is fundamentally different. Specifically, for thin films, the dipolar nanoparticle LSPR interacts with the film plasmons and forms two resonances. To facilitate the discussion of this effect, we here focus on the contribution from bonding film plasmons with symmetric charge alignment on the two surfaces of the film, however, the higher energy antibonding film plasmons also play a role. Although the nanoparticle plasmons in principle can couple to film plasmons of arbitrary wavelength, the Coulomb interaction is largest for film plasmons whose half wavelengths are larger than the diameter of the nanoparticle ($\lambda_{SPP} > 2D$), so that the charges on the opposite sides of the junction can align efficiently (see Fig. 1). In the terminology of the Anderson impurity model,[9,10] the higher energy resonance is a localized state (LS) above the continuum and is essentially a screened nanoparticle LSPR where the film plasmons align their surface charges with respect to the surface charges of the nanoparticle. Due to the energy mismatch between the nanoparticle LSPR and film plasmons of long wavelengths, the interaction is relatively weak and the screening is predominantly mediated by higher energy short wavelength film plasmons ($\lambda_{SPP} = 2D$), as illustrated in Fig. 1. Since such film plasmons are only weakly dependent on the film thickness, the LS does not depend strongly on the film thickness. In contrast, the low energy resonance is a "virtual state" (VS), which is induced at energies lower than the nanoparticle LSPR where the instantaneous charge polarization of the nanoparticle follows the incident field adiabatically. This state is not an eigenstate of the system and can be best described as a superposition of film plasmons of wavelengths larger than twice the diameter of the nanoparticle, as illustrated in Fig. 1. In general, such film modes would not be excited for a plane wave excitation, but are here excited because the near-field from the polarized nanoparticle couples directly to the surface charges of sufficiently long wavelength film plasmons. The largest coupling occurs for film plasmons with energies equal to the energy of the incident light, *i.e.*, longer wavelength film plasmons. Since the energies of the bonding film plasmons of long wavelength depend strongly on the film thickness, the energy of the VS is highly tunable and decreases with reduced film thickness. The field enhancements associated with the VS can be large because of the symmetric alignment of the charges of the film plasmons.[9,10]

Experimental details

The gold tips and films used in this study were prepared by evaporating gold metal (99.9999%, Nilaco) on commercially

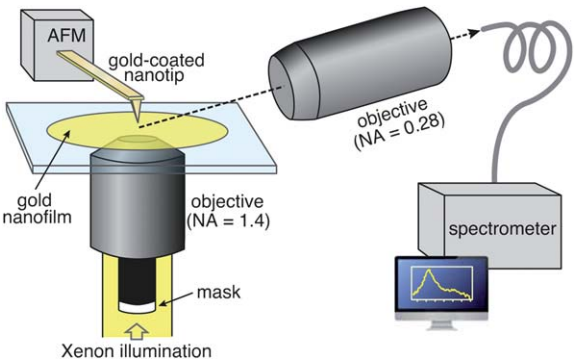

Fig. 2 Schematic illustration of the optical setup for the measurement of scattering spectra for the gold nanotip–nanofilm system.

available silicon cantilevers (CSG01, NT-MDT) of atomic force microscopy (AFM) and on clean glass coverslips, respectively, under a high vacuum of 2×10^{-7} Torr. The tip–film system was used for scattering spectra and TERS measurements.

Scattering spectra measurements

The optical setup for scattering spectra measurements, illustrated in Fig. 2, is based on an inverted optical microscope combined with a contact-mode AFM system that precisely controls the position of the tip. A gold-coated cantilever tip was placed on a gold film evaporated on a coverslip. A constant nanogap between the tip and the film was maintained through an AFM feedback system. The tip–film system was illuminated by p-polarized white light from a xenon lamp (Max 150, Asahi Spectra) through an objective lens that had a numerical aperture (NA) of 1.4 (Nikon Plan Apo). Illumination light corresponding to NA < 1 was rejected by using a mask in the illumination path. Under this configuration, a total internal reflection is achieved and a pure evanescent field is generated on the surface of the gold film. The evanescent field scatters when it interacts with the tip apex. Note that the evanescent light interacts only with the apex of the tip as it decays quickly within a nanometric distance.[19] Scattered light was collected from the side of the tip by a long-working-distance objective lens having a NA of 0.28 (Mitutoyo Plan Apo), and was detected through a liquid nitrogen cooled charge-coupled device (CCD) camera (1340 × 400 channels, −120 °C, Roper).

TERS measurements

TERS measurements were performed on monolayers of 4-aminothiophenol (4-ATP) molecules, self-assembled on gold films of different thicknesses ranging from 4 to 16 nm, and a gold-coated cantilever tip with an apex of 30 nm was brought in contact with the sample. The 4-ATP molecules were purchased from Aldrich Chemical Co., which were used without further purification. A single-mode diode laser ($\lambda = 642$ nm) was used for TERS measurements, where resonant Raman effects are negligible due to the weak absorption of 642 nm light by 4-ATP molecules. Usual optics and a CCD detector equipped spectrometer were used to record Raman spectra.

Optical measurements

The plasmonic properties of the metallic tip–film system are here experimentally studied by performing scattering spectra measurements (Fig. 2). Smooth gold thin films with thickness ranging from 4 to 20 nm were prepared as discussed before, where the roughness of each film was confirmed to be under 3 Å using AFM measurements. A gold-coated cantilever tip with apex diameter 30 nm was prepared, where the diameter of the tip apex was confirmed by scanning electron microscopy (SEM).

Fig. 3(a) shows the measured scattering spectra for various film thickness. These spectra were corrected for background signal by subtracting the spectrum obtained without the tip from the corresponding spectrum obtained with the tip. The spectra were also normalized by dividing each background-subtracted spectrum by the corresponding background spectrum. Finally, the spectra were offset on the intensity scale for facile visualization. As for a solid nanosphere on a thin film, two resonances were observed, which are the VS and the LS resonances.[9,10] Similar results are observed here for a tip–film system. For the 12 nm film, the spectrum of which is shown by (iii) in Fig. 3(a), where the peak positions were not clearly observed, a two-Lorentzian curve fitting was utilized to estimate the peak positions. The ratio of the intensities of the VS and LS modes decreases with increasing film thickness in Fig. 3(a). Fig. 3(b) shows the peak positions of the two resonances as a function of film thickness. Both peaks appear in the visible to the near-infrared region, and in particular, the VS depends strongly on the film thickness. Both the shift and relative intensities of the two resonances follow a similar pattern to what was observed in the earlier study of plasmon resonances of solid gold nanospheres on thin gold films.[9]

To further investigate the plasmonic tunability of the tip–film system, we changed the size of the tip apex. Since plasmon resonance energy in the nanosphere–film system depends on the

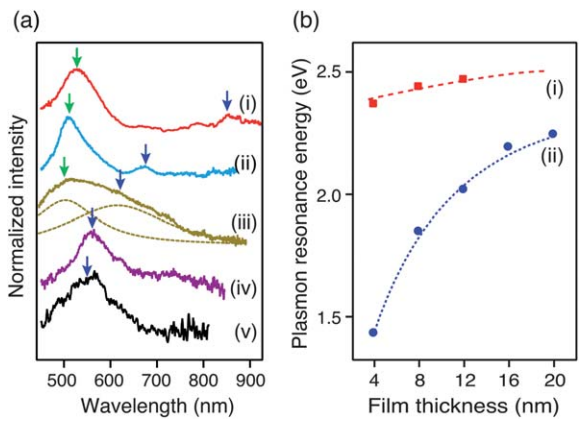

Fig. 3 (a) Scattering spectra of the gold tip–film system measured with film thicknesses of 4, 8, 12, 16, and 20 nm in curves (i)–(v), respectively. The diameter of the gold-coated nanotip was 30 nm for all spectra. The two dotted lines in (iii) represent Lorentzian fittings. The arrows indicate the plasmon resonance peaks that shift with the film thickness. (b) Plasmon resonance energy obtained from the experimental results as a function of film thickness. The squares and the circles in (i) and (ii) represent the LS and the VS modes, respectively. The dashed and dotted lines are best fits obtained by using least square exponential curves to guide the eyes.

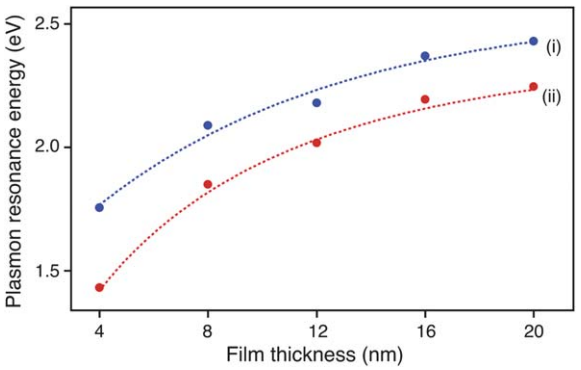

Fig. 4 Energy of VS as a function of the film thickness in the gold tip–film system for tips with apex diameters (i) 15 and (ii) 30 nm. The dotted lines are the best fits obtained by using least square exponential curves to guide the eyes.

diameter of the nanosphere,[9,10] the plasmon resonance energy in the tip–film system is also expected to depend on the size of the tip apex. A gold-coated tip with the apex diameter of 15 nm was prepared, and scattering spectra were measured from the tip–film gap using the same optical setup as before. Fig. 4 shows a comparison of the resonance peak energies of the VS modes for tips with apex diameters of 15 and 30 nm. The energies for the 15 nm tip are blue-shifted compared to the 30 nm results for all film thicknesses. Also this result is in good agreement with the previous study of gold nanospheres on thin gold films[9,11] and shows that the tunability of the metallic tip–film system can be further extended by manipulating the apex size of the tip.

Theoretical simulations

We expect the qualitative features of the interaction of a plasmonic tip with a film to be similar to the nanosphere–film system since the interactions are local. To model the system, we use the finite-difference time-domain (FDTD) method. The tip is approximated as a gold nanosphere,[30] because a gold-coated tip fabricated by the vacuum vapor deposition method forms a nanosphere structure at the tip apex. The results for a more realistic tip-like particle, such as an ellipsoid or a cone, would be qualitatively similar to that for a sphere but with plasmon energies shifted slightly to the red and with a slight increase in local electric field enhancements. In our simulation, a gold nanosphere of diameter 30 nm is placed 2 nm away from an infinite gold film of varying thickness on top of a glass substrate. The system is illuminated with a plane wave polarized perpendicular to the surface of the film (p-polarization). A grid size of 1 nm is used which ensures good convergence. The dielectric permittivity of gold and glass is taken from the literature.[31]

Fig. 5(a) shows the calculated scattering spectra for film thickness ranging from 4 to 20 nm. As expected, both the LS and VS modes are observed. Both resonances exhibit clear blueshift with increasing film thickness. The LS mode shifts from 615 to 530 nm and the VS mode from 833 to 613 nm. This wide-range tunability suggests the possibilty of precise control of the plasmon resonance energy by changing the film thickness. Fig. 5(b) shows a cross-section of the electric field distribution in the gap for the LS mode for a film thickness of 4 nm. The field

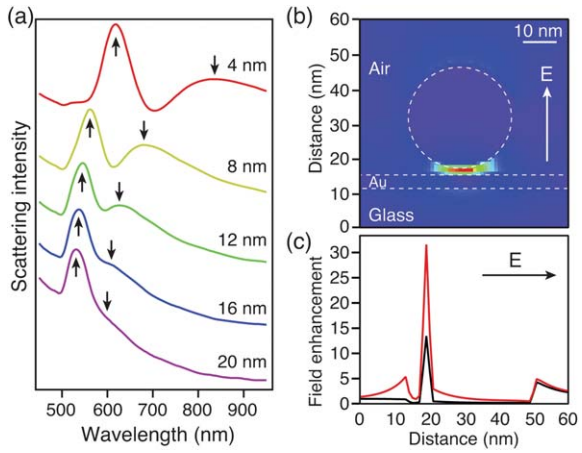

Fig. 5 (a) Calculated scattering spectra at a nanogap between a gold nanosphere and a gold nanofilm. The diameter of the gold nanosphere was fixed at 30 nm, and the spectra were calculated for the film thickness of 4, 8, 12, 16 and 20 nm. (b) Electric field distribution of the scattered light for the LS mode simulated for a 30 nm nanosphere and 4 nm film. The white dotted lines represent boundaries and the white arrow shows the field direction. (c) Line profile along the gap showing field enhancement highly confined to the gap. The red and the black curves correspond to the VS and LS modes, respectively, and the black arrow indicates the field direction.

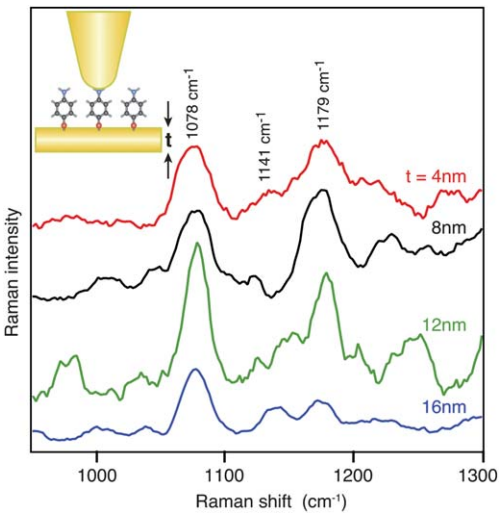

Fig. 6 Tip-enhanced Raman spectra from a monolayer of 4-ATP molecules sandwiched between a gold-coated nanotip with the apex diameter of 30 nm and gold nanofilms with indicated thicknesses. The tip–film system, together with sandwiched sample molecules, is illustrated in the inset. The excitation wavelength is 642 nm.

enhancement for the VS mode is similar. Since the field enhancements are localized to the gap, the system can be used as a local probe in TERS applications.

Tunable enhancement in TERS

We now demonstrate that by controlling the film thickness it is possible to tune the plasmon resonances to optimize the Raman signal for a given wavelength in a TERS experiment. A self-assembled monolayer of 4-ATP molecules was sandwiched between a gold-coated tip with an apex of 30 nm and gold nanofilms of different thicknesses ranging from 4 to 16 nm. The inset of Fig. 6 shows a schematic of the sample configuration. Some examples of TERS spectra measured for the film thicknesses of 4, 8, 12 and 16 nm are shown in Fig. 6. These spectra represent far-field-subtracted near-field-enhanced Raman signals. As shown in Fig. 6, Raman modes were observed at 1078, 1141 and 1179 cm^{-1}, which correspond to various vibrational modes of a 4-ATP molecule.[32] Since these spectra are near-field enhanced spectra, the appearance of these modes is due to the tip-induced electric field enhancements in the junction between the tip and the film. The spectrum measured for 12 nm-thick film shows distinctly larger enhancement at 1078 cm^{-1} compared to the spectra from both thinner and thicker films. Here we focus on the mode at 1078 cm^{-1}, because this mode is attributed to enhancement based on the electromagnetic effect alone in SERS. Thus, we can conclude that the Raman enhancement depends on the film thickness, and that the enhancement is selectively increased for specific film thickness.

In order to quantitatively evaluate the Raman enhancement and to understand its dependence on the film thickness, we calculated the enhancement factor (EF) at the gap as a function of film thickness using the standard method.[33,34] The EF can be defined as

$$\mathrm{EF} = \frac{I_{\mathrm{gap}}/N_{\mathrm{gap}}}{I_{\mathrm{bulk}}/N_{\mathrm{bulk}}} \quad (1)$$

where I_{gap} represents the enhanced intensity of a Raman mode in the TERS spectrum when the tip approaches the sample placed on the film, and I_{bulk} is the intensity of the same Raman mode in the normal Raman spectrum of the solid sample. To estimate the EF, we focus on the 7*a*-type vibrational mode of 4-ATP molecules at 1078 cm^{-1}, which is believed to be primarily due to the electromagnetic enhancement effect and not the chemical effect.[35] It is highly unlikely that the chemical effect would depend on the film thickness. N_{gap} represents the number of 4-ATP molecules within the volume of the enhanced field at the nanogap, which is estimated by the size of the enhanced field at the gap and the packing density of the sample molecules on the gold film. The lateral size of the enhanced field can be described as $L = \sqrt{dD}$,[30] where d is the gap-distance between the tip and the film and D is the diameter of the tip apex. The gap-distance is roughly assumed to be equal to the thickness of a monolayer of 4-ATP molecules (~6 Å),[36] and the packing density is ~0.20 nm^2 on full coverage of a gold film.[34] N_{bulk} is the number of 4-ATP molecules in a solid sample within the focal volume.[37] Since the density of solid 4-ATP is 1.18 g cm^{-3}, N_{bulk} can be calculated from the volume of the laser focus.

Fig. 7 shows the calculated EF from our experimental measurements discussed in Fig. 6, as a function of the film thickness, which was varied from 4 to 16 nm. The EF was averaged from twenty-five identical measurements for each film thickness. The error bars in Fig. 7 correspond to these 25 measurements and are most likely due to variations in the sample molecules packing density on the film and from temporal fluctuation of the instruments used in the optical setup. As shown in Fig. 7, the EF is maximal for a film thickness of 12 nm, which was also seen from the spectra shown in Fig. 6. As shown in Fig. 5, for a tip apex of 30 nm (also shown in the inset), for this thickness, the VS plasmon energy lies around 2.0 eV, which matches the excitation wavelength

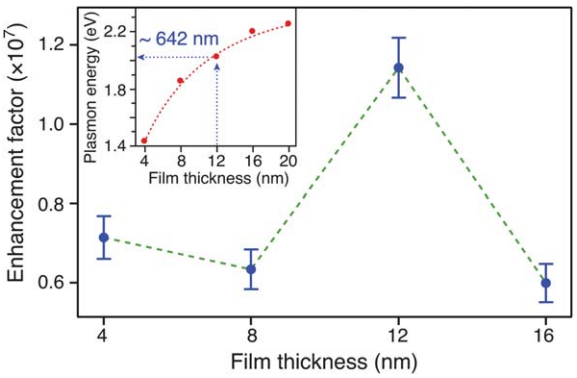

Fig. 7 Enhancement factor in TERS measurement, where the sample was placed at the nanogap of a gold tip–film system, as a function of film thickness. The error bars represent the experimental error from 25 identical measurements. The inset displays the data for a 30 nm tip apex from Fig. 5 and shows that the VS plasmon energy for a film of 12 nm thickness matches the wavelength of the incident light, $\lambda = 642$ nm.

of 642 nm. One also notices that the EF for the 4 nm film is not the smallest although the VS resonance here is expected to be the farthest from the excitation laser. We believe that this is due to the general observation that thin films provide larger electric field enhancements than thick films due to the symmetrically aligned surface charges.[10] For a thin film the surface charges on the bottom surface of the film contribute significantly to the field enhancement in the junction because of their proximity. These results indicate that, in addition to influencing the plasmon energies, film thickness also plays an important role for the magnitude of the field enhancement in the junction.

Discussion and conclusions

In conclusion, we have demonstrated experimentally and theoretically that the plasmonic response and near-field in a metallic nanotip–film junction can be tuned by varying the thickness of the film. The optical response is characterized by two resonances. The lower energy resonance is particularly sensitive to the film thickness and can be tuned over a broad range of the visible to the near infrared spectrum allowing for a precise tuning of the plasmonic response to match the incident laser light. We also show that the plasmonic response can be changed by controlling the diameter of the tip apex. The field enhancement in the tip–film junction was also studied by measuring the Raman signal in TERS on 4-ATP molecules. It was found that the TERS enhancement factors were the strongest when the film thickness was such that the wavelength of the plasmons overlapped the excitation laser. This approach of tuning the plasmon resonance energy by modulating the film thickness could provide significant improvement of the field enhancement and the spatial resolution in tip-enhanced near-field spectroscopy and microscopy.

Acknowledgements

This work was supported by a grant from the Japan Science and Technology Agency under a Core Research for Evolutional Science and Technology (CREST) project "Plasmonic Scanning Analytical Microscopy" and by the Robert A. Welch Foundation (PN) under grant C-1222.

Notes and references

1 K. Kneipp, H. Kneipp, B. Kartha, R. Manoharan, G. Deinum, I. Itzkan, R. R. Dasari and M. S. Feld, *Phys. Rev. E: Stat. Phys., Plasmas, Fluids, Relat. Interdiscip. Top.*, 1998, **57**, 6281.
2 S. Lal, S. Link and N. J. Halas, *Nat. Photonics*, 2007, **1**, 641.
3 C. Sönnichsen, B. M. Reinhard, J. Liphardt and A. P. Alivisatos, *Nat. Biotechnol.*, 2004, **22**, 883.
4 A. J. Haes, L. Chang, W. L. Klein and R. P. Van Duyne, *J. Am. Chem. Soc.*, 2005, **127**, 2264.
5 C. F. Bohren and D. R. Huffman, *Absorption and Scattering of Light by Small Particles*, Wiley, New York, 1983.
6 K. H. Su, Q. H. Wei, X. Zhang, J. J. Mock, D. R. Smith and S. Schultz, *Nano Lett.*, 2003, **3**, 1087.
7 E. Prodan, C. Radloff, N. J. Halas and P. Nordlander, *Science*, 2003, **302**, 419.
8 N. J. Halas, S. Lal, W. S. Chang, S. Link and P. Nordlander, *Chem. Rev.*, 2011, **111**, 3913.
9 F. Le, N. Z. Lwin, J. M. Steele, M. Käll, N. J. Halas and P. Nordlander, *Nano Lett.*, 2005, **5**, 2009.
10 F. Le, N. Z. Lwin, N. J. Halas and P. Nordlander, *Phys. Rev. B: Condens. Matter Mater. Phys.*, 2007, **76**, 165410.
11 P. Nordlander and F. Le, *Appl. Phys. B: Lasers Opt.*, 2006, **84**, 35.
12 S. Nie and S. R. Emory, *Science*, 1997, **275**, 1102.
13 K. Kneipp, Y. Wang, H. Kneipp, L. T. Perelman, I. Itzkan, R. R. Dasari and M. S. Feld, *Phys. Rev. Lett.*, 1997, **78**, 1667.
14 N. Hayazawa, Y. Inouye, Z. Sekkat and S. Kawata, *J. Chem. Phys.*, 2002, **117**, 1296.
15 C. C. Neacsu, J. Dreyer, N. Behr and M. B. Raschke, *Phys. Rev. B: Condens. Matter Mater. Phys.*, 2006, **73**, 193406.
16 K. F. Domke, D. Zhang and B. Pettinger, *J. Am. Chem. Soc.*, 2006, **128**, 14721.
17 W. Zhang, B. S. Yeo, T. Schmid and R. Zenobi, *J. Phys. Chem. C*, 2007, **111**, 1733.
18 B. Pettinger, K. F. Domke, D. Zhang, G. Picardi and R. Schuster, *Surf. Sci.*, 2009, **603**, 1335.
19 I. Notingher and A. Elfick, *J. Phys. Chem. B*, 2005, **109**, 15699.
20 A. Downes, D. Salter and A. Elfick, *J. Phys. Chem. B*, 2006, **110**, 6692.
21 T. Yano, T. Ichimura, A. Taguchi, N. Hayazawa, P. Verma, Y. Inouye and S. Kawata, *Appl. Phys. Lett.*, 2007, **91**, 121101.
22 N. Hayazawa, H. Ishitobi, A. Taguchi, A. Tarun, K. Ikeda and S. Kawata, *Jpn. J. Appl. Phys.*, 2007, **46**, 7995.
23 A. Cvitkovic, N. Ocelic, J. Aizpurua, R. Guckenberger and R. Hillenbrand, *Phys. Rev.Lett.*, 2006, **97**, 060801.
24 J. J. Mock, R. T. Hill, Y. J. Tsai, A. Chilkoti and D. R. Smith, *Nano Lett.*, 2012, **12**, 1757.
25 D. Y. Lei, A. I. Fernandez-Dominguez, Y. Sonnefraud, K. Appavoo, R. F. Haglund, J. B. Pendry and S. A. Maier, *ACS Nano*, 2012, **6**, 1380.
26 H. J. Li, S. L. Fu, S. X. Xie, H. Q. Xu, X. Zhou and J. J. Wu, *Sci. China, Ser. G: Phys., Mech. Astron.*, 2010, **53**, 38.
27 M. Hu, A. Ghoshal, M. Marquez and P. G. Kik, *J. Phys. Chem. C*, 2010, **114**, 7509.
28 H. J. Li, Q. Liu, S. Xie, X. Zhou and S. Fu, *Opt. Commun.*, 2009, **282**, 2845.
29 M. H. Lin, H. Y. Chen and S. Gwo, *J. Am. Chem. Soc.*, 2010, **132**, 11259.
30 R. Hillenbrand, T. Taubner and F. Keilmann, *Nature*, 2002, **418**, 159.
31 P. B. Johnson and R. W. Christy, *Phys. Rev. B: Solid State*, 1972, **6**, 4370.
32 M. Osawa, N. Matsuda, K. Yoshii and I. Uchida, *J. Phys. Chem.*, 1994, **98**, 12702.
33 Y. Wang, H. Chen, S. Dong and E. Wang, *J. Chem. Phys.*, 2006, **124**, 074709.
34 X. Hu, T. Wang, L. Wang and S. Dong, *J. Phys. Chem. C*, 2007, **111**, 6962.
35 K. Kim and J. K. Yoon, *J. Phys. Chem. B*, 2005, **109**, 20731.
36 Y. T. Kim, R. L. McCarley and A. Bard, *J. Phys. Chem.*, 1992, **96**, 7416.
37 For the estimation of the focal area, theory of Abbe's diffraction limit was utilized. The diameter of the lateral area was estimated to be ~200 nm and the penetration depth was estimated to be ~170 nm.